JOURNAL OF AIRCRAFT
Vol. 43, No. 2, March–April 2006

Classical Wing Theory and the Downward Velocity of Vortex Wakes

Vernon J. Rossow*
NASA Ames Research Center, Moffett Field, California 94035-1000

Classical wing theory is extended downstream from a flat vortex sheet to include vortex-wake configurations that can be considered as fully rolled up into a vortex pair. Classical wing theory was chosen as the method to be used because it is based on the flux of downward momentum imparted to the ambient flow field by the lift on a wing. After the theory is reviewed to establish the theoretical process used to analyze vortex wakes, it is extended to the configuration of lift-generated wakes that occur after roll-up of the vortex sheet, and that are composed of a vortex pair inside of an oval-shaped region that propagates downward as a unit. The distribution of downward momentum inside the oval, and in the surrounding fluid, found for the rolled-up vortex pair is then applied to vortex wakes as they undergo instabilities that lead to their decomposition and dispersion.

Nomenclature

AR	=	wing aspect ratio $= b^2/S_w$
b	=	wing span, ft (m)
b'	=	distance between vortex centroids, ft (m)
c	=	wing chord, ft (m)
C_L	=	lift coefficient $= L/qS$
D_i	=	lift-induced drag, lb (N)
G	=	Γ_o/bU_∞
L	=	lift, lb (N)
q	=	$\rho U_\infty^2/2$, lb/ft^2 (N/m^2)
S_w	=	wing planform area, ft^2 (m^2)
T_{en}	=	rate of transfer of kinetic energy to flow field, (ft − lb/s) (m − N/s)
T_t	=	tU_∞/b'
t	=	time (s)
U_∞	=	free-steam velocity, ft/s (m/s)
v, w	=	velocity components in y and z directions, ft/s (m/s)
Wt	=	weight of aircraft, lb (N)
x	=	distance in flight direction, ft (m)
y	=	distance in spanwise direction, ft (m)
z	=	distance in vertical direction, ft (m)
Γ	=	vortex strength, ft^2/s (m^2/s)
ρ	=	air density, slugs/ft^3 (kg/m^3)

Subscripts

∞	=	freestream condition
app	=	apparent or virtual
$c/4$	=	quarter-chord station
decomp	=	decomposing wake
o	=	centerline
oval	=	vortex oval
plate	=	flat plate configuration of vortex sheet
pr	=	vortex pair

I. Introduction

EFFORTS are under way to develop more efficient ways in which aircraft can safely avoid the vortex wakes of preceding aircraft in order to increase airport capacity.[1] Of interest in this note are the downward velocity and associated momentum distribution imparted to the wake by the lift on a wing as a function of the various stages of wake development and decay. Although the downward velocity of wakes shed by conventional aircraft is not large, reliable information on their travel velocity is needed for wake-advisory systems to keep track of the time-dependent locations of wakes, so that they can be reliably avoided. The downward velocity of lift-generated wakes becomes especially important when the generating aircraft is low enough to be in ground effect, because the descent velocity of a wake then becomes a lateral velocity, which has the potential to transport a vortex hazard to adjacent runways.

The downward motion of the wake generated by lift on a wing is usually determined by assuming that the wake consists largely of a vortex pair. Since the vortices are embedded in the air, they also move laterally with the wind, which is best determined by measuring the magnitude and direction of the wind directly. At this time, the vertical motion of a vortex pair can be measured by the use of various devices, but advanced knowledge is needed for traffic planning at airports, which requires that the downward and possible lateral transport be estimated theoretically. For that purpose, the velocity, weight, wingspan, and altitude of the aircraft are used to estimate the magnitude of the circulation contained in the vortices that form several wingspans behind the aircraft. The self-induced downward velocity of a vortex pair is then given by

$$w_{\text{pr}} = -\Gamma_o \big/ 2\pi b' \tag{1}$$

where Γ_o is the circulation contained in each vortex in the pair (which is also the centerline circulation bound in the wing), and b' is the spanwise distance between the centroids of vorticity, which is about equal to $\pi/4$ times the wingspan, b. Equation (1) applies to a wake composed primarily of a vortex pair. The aerodynamic configuration and the downward velocity of a vortex wake change considerably from the time when a vortex wake consists of a nearly flat vortex sheet at the trailing edge of the wing, through roll-up into a vortex pair, and finally through wake decomposition and dispersion, which is when the wake components are indistinguishable from ambient turbulence in the air.

For the foregoing reasons, classical wing theory is used to clarify how the motion of and downward momentum in vortex wakes change as the wake shape evolves from a flat sheet at the trailing edge of the wing to the rolled-up vortex pair farther downstream, and eventually to the wake configuration where the wake has completely decomposed. The various stages that vortex wakes go through are studied by using the relationship between the lift force on the wing and the generation of downward momentum in the wake. In the far field, where vortex wakes have become disorganized,

Received 21 December 2004; revision received 28 March 2005; accepted for publication 28 March 2005.

*Senior Staff Scientist, Mail Stop N210-10, Aerospace Operations Modeling Office. Associate Fellow AIAA.

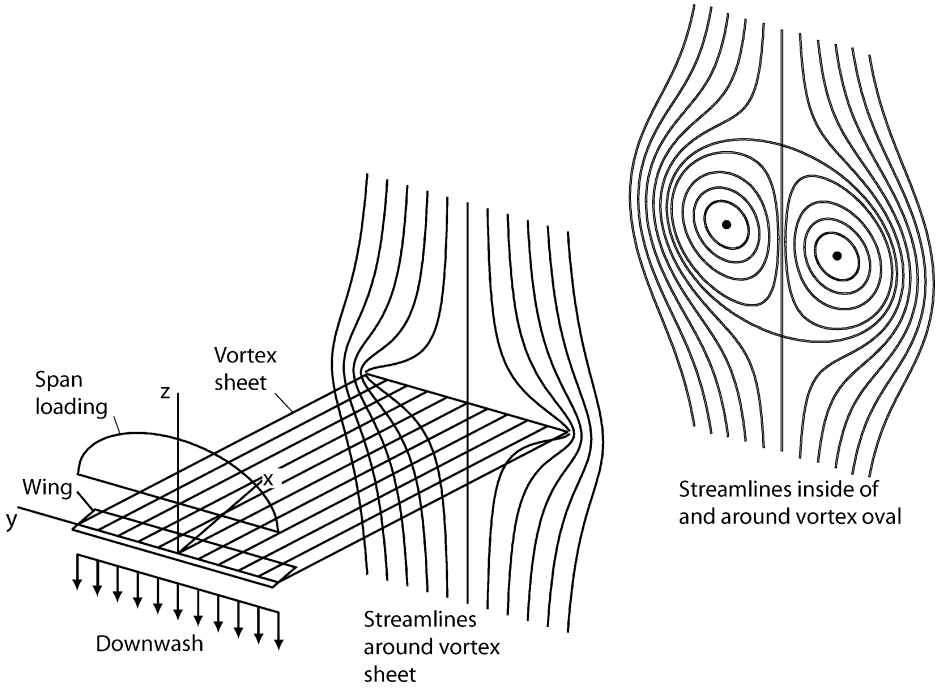

Fig. 1 Diagonal view of flow field of wing, vortex sheet, and vortex oval.

momentum considerations are used along with measurements made on the wakes of aircraft at cruise altitude to estimate the size and downward velocity of vortex wakes. It is during this time that instabilities and large-scale mixing rapidly enlarge the cross-sectional size of the wake, and the swirl velocities in the wake begin to become benign. The results presented provide improved estimates for the downward velocity of lift-generated vortex wakes to better locate the hazard posed by vortex wakes.

II. Classical Theory for Wings of Finite Span

Classical wing theory was developed in the early part of the 20th century to provide a simple and quite reliable method for understanding the concepts associated with the design of lift distributions on wings and the drag force due to lift. The associated fluid-dynamic concepts for the flowfield around lifting wings of finite span are described in a number of texts,[2–7] which are listed according to their dates of publication. Books are cited as references because the documents that originally introduced the theory are now not readily available. For readers not familiar with classical wing theory, the books written by Munk[2] and Prandtl and Tietjens[3] provide insight into the development of the theory. The other books listed as references elaborate on the details of the concept, or on the analysis used for the fluid-dynamical processes involved.

The theory developed treats the effect of finite span on the loading on the wing, its associated drag, and the distribution of downward momentum in the wake as imparted to the wake by the lift on the wing. It begins with the observation that, if a wing of finite span develops the same lift at each spanwise station, the surrounding flowfield can be represented by a single bound vortex that extends from wingtip to wingtip at about the quarter-chord line of the wing and by two semi-infinite line vortices that trail from the two wingtips.[2,6] The trailing vortices are, of course, opposite in sign, so all three segments of the vortices form a continuous-line, or horseshoe, vortex. In actual practice, wings of finite span have a gradual decrease in lift from the wing centerline to their tips, which causes vorticity to be shed all along the wing trailing edge, that is, the edge shown as trailing from the quarter-chord line in Fig. 1. The most efficient spanwise distribution of lift for a given span is elliptical, because its vortex wake induces a uniform downwash across the entire span of the wing, which has been found to produce the minimum lift-induced drag for a given wing span and total lift.[2] Because the downwash on the wing is the same over its entire span, the vortex sheet it sheds tends to remain nearly flat for a short distance behind the trailing edge of the wake-generating wing, before it begins to roll up into a vortex pair.

The classical theory for wings of finite span is based on the representation of the vortex wake shed by an elliptically loaded wing with a flat vortex sheet that trails downstream from the wing. In its original formulation,[2,3] the theory assumes that the wake is flat from the wing to far enough behind the wing so that roll-up of the sheet into a vortex pair does not influence any fluid dynamical processes going on at or near the wing. It is assumed in the theory that the vortex sheet begins along a line located at one-fourth of a chord length behind the leading edge of the wing and extends downstream to infinity. The across-wake flowfield is then analyzed at two stations along the flat vortex sheet to establish guidelines for the design of the wing. The first station is located at the leading edge of the trailing vortex sheet, which is at one-quarter of the wing chord back from the leading edge of the wing; see Fig. 1. The second station is taken at a location deemed to be far enough behind the wing (i.e., mathematically at infinity) so that the flowfield at that station is not appreciably affected by the end of the vortex sheet at the wing quarter-chord line.

In this study, a third station downstream from the second one is introduced to gain an improved understanding of the distribution of energy and downward momentum in the vortex wake when the vortex sheet is fully rolled up into a pair of counter-rotating vortices. The roll-up process (not shown in Fig. 1) actually begins at the trailing edge of the wing and then rapidly forms into the flowfield of a vortex pair inside an oval-shaped region, which also has an associated external flowfield as indicated in the figure. A segment of a flat vortex sheet behind the wing is shown in Fig. 1 between the first two stations, because it is the configuration assumed in the classical wing theory of Prandtl and Munk. More accurate computations with more complete theories indicate that the error involved is small.[8,9]

At the first station, located at the quarter-chord of the wing, the spanwise vortex bound in the wing interacts with the free-stream velocity to develop the lift force on the wing.[6] The flow field of the trailing vortex sheet induces a downwash of constant velocity, $w_{c/4}$, across the wing at its quarter-chord station. The downwash interacts with the spanwise vortex bound in the wing to produce a ratio of the lift to the corresponding lift-induced drag force, given by

$$D_i/L = w_{c/4}\big/U_\infty \tag{2}$$

where L is the lift on the wing, D_i is the lift-induced drag on the wing, U_∞ is the free-stream velocity, and $w_{c/4}$ is the magnitude of the wake-induced downwash velocity at the first station.

At the second station, the vortex sheet shed by the wing is, for theoretical purposes, again assumed to be a flat surface, even though roll-up has begun. The downward velocity of the vortex sheet is then determined by the magnitude required to accommodate the rate at which downward momentum is imparted to the fluid by the lift force on the wing. It is noted that the theory applies equally well as an accurate model of the partially rolled-up wake.[8] Because the second station is placed far downstream of the wing, the flowfield around the vortex sheet is considered as two-dimensional. The flowfield at the second station is then much easier to analyze than the three-dimensional situation at the wing quarter-chord line. Because the flat vortex sheet does not contain any fluid, the entire lift force and the downward momentum produced in the air go into the acceleration of the fluid around the downward moving flat vortex sheet, which is treated as a rigid flat plate. The rate of kinetic energy production in the flow field, T_{en}, is then the only recipient of the rate at which work is being done by the wing on the fluid, and may be written as[5–7]

$$T_{\text{en}} = D_i U_\infty = (\rho/2) A_{\text{app}} U_\infty w_{\text{plate}}^2 \tag{3}$$

where A_{app} is an effective or apparent cross-sectional area of fluid that is being deflected and accelerated downward by the lift on the wing, and w_{plate} is the downward velocity of the flat vortex sheet at station 2, which is assumed to move as a rigid flat plate. The freestream velocity, U_∞, is needed in Eq. (3) and other equations to follow to represent the rate at which downward momentum is imparted to the freestream fluid. That is, as the lifting wing moves through the fluid, it continually accelerates more and more fluid downward. The fluid accelerated downward is contained within the entire flowfield around the flat vortex sheet, and not within a given finite volume. Also, the volume of fluid involved in the process is not accelerated downward at a uniform velocity, but at a wide range of velocities in different directions to make up the flow field around the flat vortex sheet, which is shown at the second station in Fig. 1 as the flow about a rigid flat plate. However, the net downward momentum may be represented as an acceleration of a given cross section of fluid to a uniform downward velocity. The foregoing idea was labeled an apparent-mass concept by Prandtl and Munk to more easily represent the force field on the fluid. The apparent volume or mass concept applies to the generation of energy and downward momentum in the fluid to sustain the lift on the wing, as given by

$$L = \rho A_{\text{app}} U_\infty w_{\text{plate}} \tag{4}$$

An inviscid analysis of the wing as it imparts kinetic energy to the fluid surrounding a flat plate (i.e., the vortex sheet) that is moving downward is found to be given by[5]

$$T_{\text{en}} = (\rho/2)(\pi/4) b^2 U_\infty w_{\text{plate}}^2 \tag{5}$$

where b is the span of the elliptically loaded wing. Comparison of Eqs. (3) and (5) yields

$$A_{\text{app}} = (\pi/4) b^2 \tag{6}$$

which is the area of a circle having a diameter equal to the span of the wing. The parameter A_{app} is not an actual identifiable region in the flow field, but is an equivalent cross-sectional area of fluid that would need to be accelerated uniformly and continuously to obtain the same steady-state lift force. It has traditionally been called the apparent or virtual mass of the fluid motion.

The downward velocity of the vortex sheet at the second station, w_{plate}, is found by comparison of Eqs. (4) and (6) with the vortex lift generated by the interaction of the vortex bound in the wing and the freestream velocity by use of an equivalent vortex, Γ_o, over a distance in the spanwise direction equal to the distance, b', between the centroids of the two trailing vortices, as[6]

$$L = -\rho U_\infty \Gamma_o b' \tag{7}$$

where Γ_o is the centerline value of the circulation bound in the wing at its quarter chord station, and $b' = b\pi/4$ for an elliptically loaded wing. The combination of Eqs. (3–7) yields

$$w_{\text{plate}} = \Gamma_o / b \tag{8}$$

where w_{plate} is the downward velocity of the flat-plate configuration of the vortex sheet at the second station. Because the velocity field of a vortex sheet is half as large at its semi-infinite end, compared with the two-dimensional value, the downwash velocity at the quarter chord line of the wing is one-half the magnitude predicted at the second station. Therefore, at the quarter-chord line of the wing the downwash velocity is given by

$$w_{c/4} = w_{\text{plate}}/2 = \Gamma_o / 2b \tag{9}$$

The conventional relationship between the lift coefficient and the induced-drag coefficient is found from Eq. (3), after a substitution is made for w_{plate}, as

$$C_{Di} = C_L^2 \big/ \pi \mathrm{AR} \tag{10}$$

where $C_{Di} = D_i / q S_w$ and $C_L = L / q S_w$ are respectively the induced-drag and lift coefficients, $\mathrm{AR} = b^2 / S_w$ is the aspect ratio of the wing, and S_w is the planform area of the wing.

III. Extension to Vortex Oval

In the preceding section, a description was given of the method used by classical wing theory to derive relationships at two stations on a flat vortex sheet for the downward momentum in the flowfield and the lift and drag forces on the wing. The same type of analysis is now applied to a third station downstream of the second, where the vortex sheet is assumed to be fully rolled up. That is, the flowfield at the third station is treated by use of energy relationships that lead to an apparent mass representation for the energy and downward momentum in the flow field.

At first, it is surprising that neither of the two downwash velocities, w_{plate} and $w_{c/4}$, is equal to the self-induced downward velocity of a vortex pair given by Eq. (1). In fact, the downwash velocities at stations 1 and 2 are considerably larger than the self-induced downward velocity of the corresponding vortex pair expressed by Eq. (1). Although the three downward velocities are different, all three are correct for the configuration assumed for the vortex sheet at the station where they are applied. The magnitude of each depends on the distribution of circulation and on the boundary conditions specified at the three stations. That is, when the vortex sheet is constrained to be flat, its downward motion must be based on kinetic energy and downward momentum considerations for a flat plate, and not on the self-induced values for a vortex pair. The formulation needed for the flowfield of the vortex pair is now derived.

Because the flat-plate configurations of the vortex sheet at stations 1 and 2 are unstable, the individual elements of the vortex sheet in actual flow fields do not remain flat, as shown in Fig. 1. Instead, when segments of the vortex sheet are allowed to move in response to the self-induced velocities on the vortex sheet, the flat vortex sheet begins to roll up from the wingtip edges inboard to form a pair of counter-rotating vortices like those shown at the most downstream location in Fig. 1. The roll-up process is essentially complete some 3 to 10 wingspans behind the wing.

It is noted that the vortex sheet has no cross-sectional area as long as it is flat, but does occupy considerable area when the roll-up process is completed. The reason for the increase in cross-sectional area is that the swirling process of the vortex sheet envelops fluid during the roll-up process. The enveloping process is illustrated in Fig. 2 by means of a calculation based on a point–vortex representation of the vortex sheet. To establish a steady-state flow field relative to an observer, an upwardly moving stream is superimposed on the flow field. That is, for viewing purposes, the self-induced downward movement of the centroids of the port and starboard parts of the vortex sheet is just offset by an upwardly moving stream, whose magnitude is given by Eq. (1) for a vortex pair.

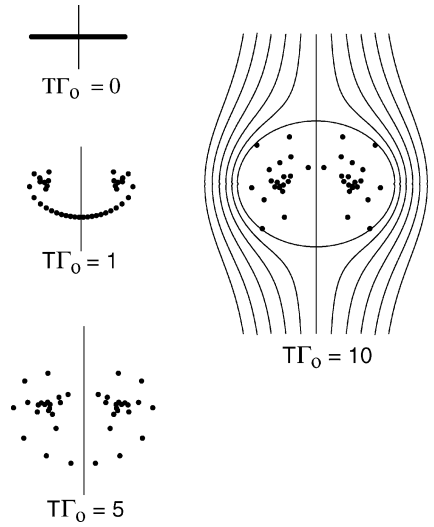

Fig. 2 Point-vortex representation of roll-up of vortex sheet to indicate how fluid is enveloped as oval is formed.

Figure 2 displays the instantaneous locations of the point vortices at four different times, but only presents the vortex oval and the streamlines around it for the final time. The streamlines about the flat plate configuration at $TG = t\Gamma_o/b^2 = 0$ are the same as shown in Fig. 1, where t is the time. The motion of the individual vortex elements at $TG = 1$ and 5 show how, during the roll-up process, the induced motion of the vortex elements is such that they swing outboard from the centerline to gather in or envelope a large amount of fluid. At the largest time shown, $TG = 10$, the swirling motion of the point vortices causes them to be distributed throughout the vortex oval so that the streamline pattern inside and outside eventually becomes the same as that shown on the right-hand side of Fig. 1 for a fully developed vortex pair. The computations shown in Fig. 2 illustrate the sweeping or enveloping action that occurs during roll-up of the vortex sheet. This motion not only distributes vorticity throughout the oval-shaped region, but also increases the resulting size of the vortex oval from an initial vanishingly small cross-sectional area of the flat vortex sheet to a spanwise size that is just over a factor of 2 (breadth $= B_{\text{oval}} = 2.08725379b'$ and depth $= D_{\text{oval}} = \sqrt{3}b'$). The cross-sectional area is then much larger than the apparent-mass cross-section associated with the flow field at the second or flat-plate station.[4] When the vortex sheet has fully rolled up, the motion of the vortex elements becomes stable as a vortex pair inside the oval-shaped region. According to inviscid theory, the vorticity or circulation that was originally in the flat vortex sheet now surrounds the centroids of the two vortices and is entirely located within the oval. It remains then to determine how the generation of downward momentum due to the lift force on the wing is absorbed and distributed in the flow field of the vortex pair.

It is first observed that, as far as downward momentum is concerned, the body of fluid inside the oval can be treated as if it moves with the oval at the downward velocity of the vortex pair, w_{pr}. Such an assumption is quite precise because momentum varies linearly with velocity so that the average downward velocity of the body of fluid inside the oval provides the same downward momentum as an integration of local velocity over the vortex oval cross section. In addition, a streamwise distance must be chosen for the momentum computation, because the volume flow rate of fluid must be identified. As with the foregoing analysis, the streamwise-depth dimension of the slab of fluid being analyzed is based on the freestream velocity, U_∞, the equation for momentum takes on a rate at which momentum, or work, is imparted to the fluid as a response to the lift force. For this reason, the various momentum relationships include the free-stream velocity and a downward velocity.

The increment of downward momentum per unit of time that is imparted to the fluid inside the oval is therefore written as

$$\Delta M_{\text{oval}} = \rho A_{\text{oval}} U_\infty w_{\text{pr}} \tag{11}$$

where A_{oval} is the cross-sectional area of the vortex oval that contains the vortex pair. As a first estimate, the shape of the oval is approximated by an elliptical shape so that its cross-sectional area is given by

$$A_{\text{oval}} \approx B_{\text{oval}} D_{\text{oval}} \pi/4 \tag{12}$$

Comparison of the downward momentum needed to account for that generated by the lift on the wing shows that the amount expressed by Eq. (11) is less than half of the amount needed. Therefore, the fluid exterior to the oval must contain the rest of the downward momentum in some way to account for the remainder of the lift on the wing.

The way that the exterior fluid contributes to the flux of downward momentum is through the energy required to establish the flow field around the downward moving oval, in the same way it was determined for the flat vortex sheet at the second station. At the third station where the vortex oval is located, the body driving the fluid is the elliptically shaped oval that contains the vortex pair. Fortunately, the evaluation is quite simple because the corresponding energy and momentum relationships have been derived by Streeter[5] and others on the basis of the apparent-mass concept. It is found that the apparent mass volume rate that corresponds to elliptically shaped cylinders depends only on the breadth of the cross-section of the body. The apparent-mass cross-section of the oval, $A_{\text{ov-app}}$, then depends only on the breadth of the body dimension perpendicular to the direction of motion, and can be expressed in the same form as Eq. (5) by

$$A_{\text{ov-app}} = (\pi/4) B_{\text{oval}}^2 \tag{13}$$

where B_{oval} is the breadth dimension of the vortex oval, which is known quite precisely. The contribution to the rate of generation of downward momentum in the fluid exterior to the oval is then given by

$$\Delta M_{\text{ext}} = \rho(\pi/4) B_{\text{oval}}^2 U_\infty w_{\text{pr}} \tag{14}$$

Combination of the two contributions to the rate of generation of total downward momentum is given by Eqs. (11) and (14) to yield

$$M_{\text{tot}} \approx \rho(\pi/4) U_\infty w_{\text{pr}} \left(B_{\text{oval}} D_{\text{oval}} + B_{\text{oval}}^2 \right) \tag{15}$$

The total rate at which downward momentum is generated, as predicted by Eq. (15), should be in exact agreement with the rate at which downward momentum is imparted to the fluid by the lift force on the wing, as given by

$$M_{\text{lift}} = \rho(\pi/4) b^2 U_\infty w_{\text{plate}} \tag{16}$$

However, numerical results for M_{tot} and M_{lift}, show that the two values for downward momentum are not exactly equal, but differ by a small amount (0.352%) that would not matter for most engineering purposes. The difference could, however, be important for other reasons. To resolve the discrepancy, it is reasoned that all of the quantities used in the equation for downward momentum are soundly based, except in Eq. (12), where the area of the oval is approximated by an ellipse, even though the major and minor axes for the oval shape are reliable. If all of the quantities used in the momentum equations are taken as reliable except for the cross-sectional size of the vortex oval, the equality can be used to calculate a more reliable size for the oval. When this is done, it is found that

$$A_{\text{oval}} = 1.0077848 B_{\text{oval}} D_{\text{oval}} \pi/4 \tag{17}$$

is the equation that should have been used for the cross-sectional size of the vortex oval, rather than that of an equivalent ellipse. When the adjustment indicated by Eq. (17) is made to the area of the vortex oval, the rate of generation of downward momentum in the fluid is in agreement with the lift force on the wing. In addition, the downward velocity of the vortex pair and its oval are predicted exactly by Eq. (1) until the fluid dynamic structure of the flow field of the vortex pair begins to decompose.

IV. Downward Velocity During Wake Decomposition

The foregoing analysis makes it possible to estimate the descent rate of the oval after the wake has rolled up, and as it decomposes to a harmless level. As mentioned previously, the structure of a rolled-up vortex pair is stable to across-stream disturbances. If vortex pairs were also stable against longitudinal disturbances, vortex wakes would persist for long periods of time. However, it has been observed that lift-generated vortex pairs are unstable to disturbances that vary along the vortex axes. The most influential of these instabilities causes a vortex pair to develop sinusoidally shaped waves along the vortices that are around 5 to 10 wingspans in length with an optimum at $8.6b'$ or $6.8b$ (Ref. 10). As the amplitude of the waves grows, the plane of the waves also rotates about 45° so that the lower parts or troughs of the waves eventually touch and join to form irregularly shaped loops of vortex filaments. As time progresses, the loops of vorticity become even more sinuous so that the organized flow field of the vortex pair breaks down into large-scale mixing. The mixing also causes the cross-sectional size of the vortex oval to grow rapidly in size with time by a factor of 3 to 5. When this instability process has been completed (at about 1–2 min after the wake was generated), large-scale mixing has increased the size of the oval and reduced the organized swirling velocities inside the oval by an amount large enough so that the wake no longer poses an in-trail hazard to following aircraft.[11] It can, however, still pose an across-trail hazard.

An estimate of the descent velocity of the vortex oval as a function of time during the decomposition and spreading process may be obtained by use of the relationships derived in the previous section for vortex ovals, and some observations made of the size of condensation trails shed by aircraft flying at cruise altitudes.[11] The measurements indicate that the breadth of vortex ovals after roll-up and during spreading of the wake may be approximated by

$$B_{\text{decomp}}(t) \approx 0.5b\sqrt{t} \tag{18}$$

where the time, t, is the age of the wake in seconds. Equation (15) indicates that the rate of generation of downward momentum is proportional to the first power of the downward velocity, and to the second power of the breadth of the vortex oval, which is like the area of the oval. Because the lift on the aircraft is not a function of time, the generation of downward momentum must also be constant along the wake. As a consequence, the downward velocity of lift-generated wakes after roll-up of the vortex sheet and during the decomposition and decay of the wake is roughly inversely proportional to the first power of time, or in equation form,

$$w_{\text{decomp}} \approx w_{\text{pr}}(B_{\text{oval}}/B_{\text{decomp}}(t))^2 \tag{19}$$

where $B_{\text{oval}} \approx 2.08\pi b/4$. For example, due to the long-wave instability, the breadth of vortex wakes increases to about $4b$ or $5b$ during the first minute of its existence. According to Eq. (19), the downward velocity of the wake should then slow by a factor of 4 or 5. For example, if the wake-generating aircraft is in the heavy category, the downward velocity of its wake would go from somewhere between 5 to 10 ft/s to about 1 to 2 ft/s, which is in agreement with measurements taken behind aircraft.[12] Inconsistencies in the time required for the long-wave instability to begin and to go to completion make it impossible to define wake descent velocity more accurately with a simple function of time.

It can also be reasoned that the spanwise distance between centroids of vorticity would grow in proportion to the breadth of the oval and the downward velocity would decrease according to Eq. (1). A result consistent with the estimate made by the momentum rule in the previous paragraph is achieved when it is recognized that the downward impulse of the vortex pair must remain constant with time.[4] That is, due to large-scale mixing between the two sides of the wake, the vortex oval grows in size so that the centroids of vorticity are spread further apart, and the vortex strengths decrease because of the large-scale across-centerline mixing that occurs. As a result, the downward impulse in the wake as manifested by the product of the vortex strength and the spanwise distance between their centroids remains the same. Therefore, the downward velocity predicted by both the strictly momentum and the vortex self-induced method are the same. Both methods then predict that the descent velocity of the vortex oval decreases inversely with the first power of time. It is noted that both of the two foregoing arguments for downward velocity require experimental confirmation for the structure of the flow field inside of the vortex oval at times after the turbulence from the long-wave instability has gone to completion.

V. Conclusions

Classical wing theory is extended to a third downstream station where the vortex sheet has rolled up into a pair of vortices that convect downward inside an oval-shaped region. It is found that relationships derived for the rates at which energy and downward momentum are imparted to the flowfield by the lift and drag forces on the wing must include contributions from both the regions interior and exterior to the vortex oval if the entire influence of the lift force on the flowfield is to be correctly represented. It is now possible to connect the processes at the two forward stations used in classical wing theory to the processes and conditions at a third station where rollup of the lift-generated vortex sheet has been completed. After the vortex pair has been formed, vortex instabilities and large-scale mixing occur. These processes disorganize and spread the energetic parts of the wake so that the vortical regions gradually become less hazardous, and eventually become indistinguishable from naturally occurring turbulent air motions in the atmosphere. During this last stage of wake dynamics, the breadth of the vortex oval grows approximately as the square root of time, and the descent velocity is predicted to slow inversely as the first power of time.

References

[1]Rossow, V. J., "Use of Individual Flight Corridors to Avoid Vortex Wakes," *Journal of Aircraft*, Vol. 40, No. 2, 2003, pp. 225–231.

[2]Munk, M. M., *Fundamentals of Fluid Dynamics for Aircraft Designers*, The Ronald Press Co., New York, 1929, pp. 89–103.

[3]Prandtl, L., and Tietjens, O. G., *Applied Hydro- and Aeromechanics*, 1st ed., translated by J. P. Den Hartog, McGraw–Hill, New York, 1934, pp. 170–173, 185–213.

[4]Lamb, Sir Horace, *Hydrodynamics*, 6th ed., Dover, New York, 1945, p. 592.

[5]Streeter, V. L., Fluid Dynamics, McGraw–Hill, New York, 1948, pp. 126–129.

[6]Glauert, H., *The Elements of Aerofoil and Airscrew Theory*, 2nd ed., Cambridge Univ. Press, London, 1949, pp. 125–155.

[7]Kuethe, A. M., and Schetzer, J. D., *Foundations of Aerodynamics*, Wiley, New York, 1950, pp. 88–113.

[8]Smith, S. C., "A Computational and Experimental Study of Non-Linear Aspects of Induced Drag," NASA TP-3598, Feb. 1996.

[9]Smith, S. C., Kroo, I. M., "Induced Drag Computations on Wings with Accurately Modeled Wakes," *Journal of Aircraft*, Vol. 34, No. 2, 1997, pp. 253–255.

[10]Crow, S. C., "Stability Theory for a Pair of Trailing Vortices," *AIAA Journal*, Vol. 8, No. 12, 1970, pp. 2172–2179.

[11]Rossow, V. J., and James, K. D., "Overview of Wake-Vortex Hazards During Cruise," *Journal of Aircraft*, Vol. 37, No. 6, 2000, pp. 960–975.

[12]Condit, P. M., and Tracy, P. W., "Results of the Boeing Company Wake Turbulence Test Program," *Aircraft Wake Turbulence and its Detection*, 1st ed., edited by J. H. Olsen, A. Goldburg, and M. Rogers, Plenum, 1971, pp. 473–508.